International Journal for Housing Science and Its Applications
Publish August 6, 2025. Volume 46, Issue 3 Pages 7113-7123

https://doi.org/10.70517/ijhsa463611

Stability study of nonlinear system of electrical intelligent control platform based on controlling Lyapunov function

Yuhang Liu[1,*]
[1] School of Intelligent Equipment, Shandong University of Science and Technology, Tai'an, Shandong, 271001, China
Corresponding authors: (e-mail: chengyuhang1028@163.com).

Abstract Intelligent control technology is gradually becoming a key force to promote the performance improvement of electrical engineering systems. In this paper, for the nonlinear system with serious state time lag, vector Lyapunov function is constructed to relax the traditional single-function constraints and realize the flexible analysis of the stability of multiple subsystems. According to the current tracking requirement of MMMC converter, the Lyapunov controller is designed to realize the current stability control. Combined with the segmented linear approximation method, the complex nonlinear functions are decomposed into multi-domain linear combinations to reduce the complexity of controller design. The results show that the Lyapunov function can balance the convergence speed and convergence stability when the controller parameters α are taken as 0.95 and β is taken as 2. Under the influence of external event triggering mechanism, the nonlinear system equilibrium point of Lyapunov function controller remains asymptotically stable after 5s. Under the influence of faults, the trajectory of the system controlled based on the Lyapunov function controller can still return to the stability domain.

Index Terms lyapunov function, nonlinear intelligent control, single function constraint, segmented linear approximation, electrical system

I. Introduction

With the rapid development of science and technology and the increasing demand for convenience and efficiency, intelligent control platforms play an increasingly important role in electrical engineering [1]. Intelligent control platform uses advanced technical means and intelligent algorithms to realize automated control and intelligent management of electrical systems. Specifically, compared with the traditional manual control, the intelligent control platform can quickly respond and accurately control the electrical system through real-time monitoring and intelligent algorithm operation, which can improve the control precision and efficiency and minimize human error [2]-[4]. In addition, the intelligent control platform has the characteristics of automation and intelligence, which can timely judge and warn the abnormal situation of the electrical system and take corresponding measures to protect it, improve the safety and stability of the electrical system, and reduce the potential safety hazards [5]-[7]. Moreover, the intelligent control platform realizes the effective use and saving of energy by optimizing the control algorithm and adjusting the operating parameters of the equipment, intelligently adjusts the switching state and power of the equipment according to the actual demand, and reduces the energy consumption and operating costs [8]-[10]. With the development of new power systems driven by renewable energy sources, their nonlinear problems are worthy of attention. The main performance is that, compared with the traditional power system, the nonlinear characteristics of generators and electronic power equipment cause the new type of power system to produce harmonics, voltage interruption, three-phase imbalance, low system inertia, and interference resistance, which affects the stability of the electrical intelligent control platform [11]-[14].

Lyapunov function is an important tool used to study the stability of the system, which can be used to test the ability of the system to withstand external disturbances, as well as the likelihood of the system oscillation phenomenon. Since the Lyapunov function measures the stability of a system's state points, it can be used to implement control strategies to prevent system oscillations [15], [16]. The Lyapunov function can be used as an important component in an intelligent control system, which is able to efficiently detect and correspond to external environmental factors, and then convert the external environmental factors into control commands in order to regulate the system's state [17], [18].

In this paper, Lyapunov function is introduced to realize the stability control of nonlinear system of electrical intelligent control platform. Focusing on the nonlinear dynamic characteristics of the electrical intelligent control platform, the vector Lyapunov function is integrated to optimize the system stability analysis capability. Design the Lyapunov function current controller, propose the switching control strategy based on the energy function, and

balance the convergence speed and stability through parameter optimization. Combining the segmented linear approximation method and the event triggering mechanism, the stability of the nonlinear system under the control of Lyapunov function controller is verified.

II. Stability analysis of nonlinear systems based on Lyapunov functions

This part analyzes how to combine Lyapunov functions to design controllers for stabilizing control of nonlinear systems in electrical intelligent control platforms.

II. A. Asymptotic stabilization control of time-lagged nonlinear systems based on Lyapunov functions

II. A. 1) Description of the problem

In this section, the following nonlinear system model of an electrical intelligent control platform with state time lag is considered:

$$\begin{cases} \dot{x}_1(t) = c_1(t)x_2(t) + F_1(\bar{x}_1(t), \bar{x}_1(t-d_1(t))) \\ \dot{x}_i(t) = c_i(t)x_{i+1}(t) + F_i(\bar{x}_i(t), \bar{x}_i(t-d_i(t))) \\ \vdots \\ \dot{x}_n(t) = c_n(t)u(t) + F_n(\bar{x}_n(t), \bar{x}_n(t-d_n(t))) \end{cases} \tag{1}$$

where $\bar{x}_i(t) = [x_1(t), \cdots, x_i(t)]^T \in R^i$ denotes the state variables of the nonlinear system of the electrical intelligent control platform, $u \in R$ denotes the inputs to the functional controller, and for any $i = 1, \cdots, n$, $F_i(\cdot,\cdot): R^{2i} \to R$ is a continuous nonlinear function where $F_i(0,0) = 0$, $c_i(t)$ denotes the unknown time-varying control coefficients with a known control direction and there exists a known positive constant $\underline{c}_i, \bar{c}_i$ to satisfy $0 < \underline{c}_i \le |c_i(t)| \le \bar{c}_i$. Without loss of generality, it is assumed that $c_i(t)$ is positive for all $t \ge 0$ times.

This is explained below for the nonlinear function assumptions used.

Assumption 1: For $i = 1, \cdots n$, there exists a known non-negative constant h, λ such that

$$\left|F_i(\bar{x}_i(t), \bar{x}_i(t-d_i(t)))\right| \le h\sum_{j=1}^{i}\left|x_j\right| + \lambda\sum_{j=1}^{i}\left|x_{jd}\right| \tag{2}$$

where $\forall x_{jd}, x_j \in R$, $1 \le j \le i$, $\bar{x}_i(t-d_i(t)) = \bar{x}_{id}$ and $d_i(t) \in [0, \tau]$.

Note 1: System (1) is a lower triangular strict feedback system with state time lag, and many dynamical models of physics can be transformed into such structures by certain transformations, such as robotic arm systems, chemical reactor systems, and interconnected motor systems. In the current environment, the design of a simple controller for such systems and the selection of appropriate controller parameters are the focus of this section in order to further conserve energy and seek the minimum control energy.

The control objective of this section is to design an asymptotically stabilizing controller for a nonlinear system with state time lags in the system to ensure that the various states and inputs of the closed-loop system converge asymptotically to the zero equilibrium point.

II. A. 2) Main theorems and proofs

In this section, an asymptotic stability theorem based on vector Lyapunov functions is presented, which provides a new approach to asymptotic stability analysis and lays the foundation for subsequent controller design and stability analysis. Consider the following time-lagged system:

$$\begin{aligned} \dot{\varphi} &= \phi(\varphi, \varphi_t), t \ge 0 \\ \varphi(t) &= \gamma(t), \gamma \in C_d \end{aligned} \tag{3}$$

where C_d denotes the spatial domain of the continuous function $[-d, 0] \to R^n$ and $\varphi(t) \in D \subseteq R^n$ denotes the instantaneous state vector. The definition of $\|\cdot\|_d$ is as follows: $\gamma\|_d = \max_{\tau\in[-d,0]}\| gamma(\tau)\|$ where $\gamma \in C_d$. $\varphi_t \in C_d$ is denoted as the state of the time-lagged system at the moment of delay t, i.e., when there is $\tau \in [-d, 0]$ for $d > 0$ and $\phi: C_d \to R^n$ is denoted as $\varphi_t = \varphi(t+\tau)$. The origin of the system is assumed to be its equilibrium, that is, for all $t \ge 0$ there is $\phi(0,0) = 0$ and $\varphi(t, \gamma)$ denotes the system solution of the initial function C_d. Also, the following notations are used to denote the variables $V, V := V(\varphi(t)), V_{t+\tau} := V(\varphi(t+\tau))$ respectively.

Theorem 1: For the electrical intelligent control platform nonlinear system (3), there exists a continuously differentiable vector function $V=[V_1,\cdots,V_n]^T$, where $V(0)=0$, a positive definite scalar function $Q^TV(\varphi),\varphi\in D$, and positive vector $Q\in R^n_{\geq 0}$. The function $p\in K$ satisfies $p(m)>m$ for all $m>0$.

$$\max_{\tau\in[-d,0]} V_{t+\tau}\leq p(V)\Rightarrow\frac{\partial V}{\partial\varphi}\phi(\varphi,\varphi_t)\leq W\left[V_1(\varphi),\cdots,V_n(\varphi)\right]^T \tag{4}$$

Eq. $W\in R^{n\times n}$ matrix is Hurwitz's. Moreover, it satisfies the property that the diagonal elements are negative and the other elements are non-negative, then the electrical intelligent control platform nonlinear system (3) is asymptotically stable at the origin.

PROOF: The comparison system is given as follows:

$$\dot{\eta}(t)=W\eta(t),\eta(0)=\eta_0,t\geq 0 \tag{5}$$

where $\eta_0\in R^n_+$. In particular $W\eta(t)$ in Eq. (5) belongs to the set ϖ and is strictly nonnegative, so that for any nonnegative initial condition Eq. (5) has a nonnegative solution. Since $W\in R^{n\times n}$ is strictly nonnegative and Helvetic, there is a positive vector $\hat{Q}\in R^q_+$ and $\grave{o}\in R^q_+$ that satisfies the following equation

$$0=W^T\hat{Q}+\grave{o} \tag{6}$$

Then, assuming that the Lyapunov function is $v(\eta)=\hat{Q}^T\eta$, $\eta\in R^n_+$, the positive definite function $v(\eta)$ is chosen to satisfy $v(0)=0$, $\eta\in R^n_+$ and radially unbounded. Let $\beta=\min\{\grave{o}_i\}$, $\gamma=\max\left\{\hat{Q}_i\right\}$, $i=1,\cdots,n$, where $\grave{o}_i$ and $\hat{Q}_i$ are the i th component of $\grave{o}\in R^q_+$ and $\hat{Q}\in R^q_+$ respectively.

$$\begin{aligned}\dot{v}(\eta)&=\hat{Q}^TW\eta=-\varepsilon^T\eta\leq-\frac{\beta}{\gamma}\gamma\left(\sum\nolimits_{i=1}^n\eta_i\right)\\&\leq-\frac{\beta}{\gamma}\left(\sum\nolimits_{i=1}^n\gamma\eta_i\right)\leq-\frac{\beta}{\gamma}(v(\eta))\\&=-\varsigma(v(\eta)),\eta\in R^n_+\end{aligned} \tag{7}$$

Eq. $\varsigma=\frac{\beta}{\gamma}$. It can be seen that the second condition of Lyapunov-Razumikhin is fulfilled, i.e.

$$\dot{v}(\eta)\leq-\varsigma(v(\eta))\ \square\ \dot{V}(\varphi)\leq-\varsigma\left(\|\varphi\|\right) \tag{8}$$

Immediately after equation (4) is transformed into the following inequality

$$\max_{\tau\in[-d,0]} V_{t+\tau}\leq p(V)\Rightarrow\dot{V}(\varphi)\leq-\varsigma\left(\|\varphi\|\right) \tag{9}$$

System (3) is asymptotically stable at the origin. The proof is complete.

Note 2: For system (3), the theorem illustrates a new approach to asymptotic stability analysis, i.e., the asymptotic stability theorem based on the vector Lyapunov function method, which allows the use of multiple Lyapunov functions to analyze each sub-system during the stability analysis process, which, in turn, provides a flexible mechanism for relaxing the constraints, making the stability analysis process easier and more Efficient.

II. B.Lyapunov function controller design for MMMC current

Let the capacitor voltage of each bridge arm cascade submodule be stabilized at U_c, then:

$$u_{xy}=\frac{U_c}{K}\sum_{i=1}^{K}s_{xyi} \tag{10}$$

where, u_{xy} is the voltage of each bridge arm; S_{xyi} is the switching function of sub-module i; K is the number of sub-modules in cascade of each bridge arm; $x=a,b,c$, $y=r,s,t$.

It is obtained from the input $\alpha\beta 0$ transformation process followed by dq transformation:

$$\begin{bmatrix} u_{md} \\ u_{mq} \end{bmatrix} = R_m \begin{bmatrix} i_{md} \\ i_{mq} \end{bmatrix} + \left(L_m + \frac{L_{qb}}{3} \right) \begin{bmatrix} \frac{d}{dt} & -\omega_m \\ \omega_m & \frac{d}{dt} \end{bmatrix} \begin{bmatrix} i_{md} \\ i_{mq} \end{bmatrix} + \sqrt{\frac{1}{3}} \frac{U_c}{K} \begin{bmatrix} S_d \\ S_q \end{bmatrix} \tag{11}$$

where, u_{md}, u_{mq}, i_{md}, i_{mq} are the input voltage currents $u_{m\alpha}$, $u_{m\beta}$, $i_{m\alpha}$, $i_{m\beta}$ on the d, q axes; S_d, S_q are the components of the switching function in the d, q axes, respectively; ω_m is the angular frequency of the three-phase power supply voltage on the input side $\left(\omega_m = 2\pi f_m, f_m = 45/4\ Hz\right)$.

According to the sub-switching function and the relationship between the sub-module current and the module capacitance voltage, it can be obtained:

$$\frac{dU_c}{dt} = \frac{Ki_{xy}}{C} \sum_{i=1}^{K} S_{xyi} \tag{12}$$

where, C is the value of sub-module capacitance; i_{xy} is the current flowing through the xy bridge arm.

There is no current loop between the center points n, and N of the MMMC converter inputs and outputs, so $i_{nN} = 0$. The $\alpha\beta 0$ transformation followed by the dq transformation of Eq. (12) gives:

$$\frac{C}{K} \frac{dU_c}{dt} = \frac{1}{2} \left(S_d i_{md} + S_q i_{mq} \right) \tag{13}$$

can be obtained from Eqs. (11) and (13):

$$\begin{cases} L_{eq} \dfrac{di_{md}}{dt} + R_m i_{md} - \omega_m L_{eq} i_{mq} + \dfrac{S_d}{K} U_c = U_{md} \\ L_{eq} \dfrac{di_{mq}}{dt} + R_m i_{mq} + \omega_m L_{eq} i_{md} + \dfrac{S_q}{K} U_c = U_{mq} \\ \dfrac{C}{K} \dfrac{dU_c}{dt} = \dfrac{1}{2} \left(S_d i_{md} + S_q i_{mq} \right) \end{cases} \tag{14}$$

Among them:

$$S_d = S_d^* + \Delta d, S_q = S_q^* + \Delta q, L_{eq} = L_m + L_{qb}/3 \tag{15}$$

where, S_d, S_q are switching function d, q axis components, respectively; S_d^*, S_q^* are the S_d, S_q steady-state values of the d, q axis components, respectively; Δd, Δq are the S_d, S_q fluctuation values of the d, q axial components, respectively; and L_{eq} is the equivalent inductance.

In order to generate the compensation voltage and reduce the input voltage unbalance, the current of the controller in this paper is required to track the given value of the input side current. Equation (16) should be satisfied when the input side current is stabilized at the given current.

$$\begin{cases} L_{eq} \dfrac{di_{md}^*}{dt} + R_m i_{md}^* - \omega_m L_{eq} i_{mq}^* + \dfrac{S_d^*}{K} U_c^* = U_{md} \\ L_{eq} \dfrac{di_{mq}^*}{dt} + R_m i_{mq}^* - \omega_m L_{eq} i_{md}^* + \dfrac{S_q^*}{K} U_c^* = U_{mq} \\ \dfrac{C}{K} \dfrac{dU_c^*}{dt} = \dfrac{1}{2} \left(S_d^* i_{md}^* + S_q^* i_{mq}^* \right) \end{cases} \tag{16}$$

where i_{md}^*, i_{mq}^*, S_d^*, and U_c^* are the command values of i_{md}, i_{mq}, S_d, and U_c, respectively.

To model the Lyapunov function, the state variable $x = [x_i](i = 1,2,3)$ of this system.

$$x_1 = i_{md} - i_{md}^*, x_2 = i_{mq} - i_{mq}^*, x_3 = U_c - U_c^* \tag{17}$$

where x_1, x_2, x_3 are the three state variables of the system, respectively.

Then the Lyapunov function model of the system can be obtained from Eqs. (16) and (17) as:

$$\begin{cases} L_{eq}\dot{x}_1 = -R_m x_1 + \omega_m L_{eq} x_2 - \sqrt{\frac{1}{3}}\frac{x_3}{K}S_d^* - \sqrt{\frac{1}{3}}\frac{1}{K}\left(x_3 + U_c^*\right)\Delta d \\ L_{eq}\dot{x}_2 = -R_m x_2 - \omega_m L_{eq} x_1 - \sqrt{\frac{1}{3}}\frac{x_3}{K}S_q^* - \sqrt{\frac{1}{3}}\frac{1}{K}\left(x_3 + U_c^*\right)\Delta q \\ C\dot{x}_3 = \frac{1}{2}\left(x_1 S_d^* + \Delta d\left(x_1 + i_{md}^*\right) + x_2 S_q^* + \Delta q\left(x_2 + i_{mq}^*\right)\right) \end{cases} \tag{18}$$

According to the basic theory of Lyapunov function control, the system must have global asymptotic stability when the following four conditions are satisfied: 1) when $\|x\| = 0$, $V(0) = 0$; 2) when $\forall\|x\| \neq 0$, $V(x) > 0$; 3) when $\forall\|x\| \neq 0$, $\dot{V}(x) < 0$; 4) when $\|x\| \to \infty$, $V(x) \to \infty$.

Assuming that the Lyapunov energy function of this system is chosen $V(x)$ for:

$$V(x) = \frac{1}{2}L_{eq}x_1^2 + \frac{1}{2}L_{eq}x_2^2 + \sqrt{\frac{1}{3}}\frac{C}{K}x_3^2 \tag{19}$$

Derivation of Eq. (19) yields:

$$\dot{V}(x) = x_1 L_{eq}\dot{x}_1 + x_2 L_{eq}\dot{x}_2 + \sqrt{\frac{1}{3}}\frac{2x_3 C}{K}\dot{x}_3 \tag{20}$$

This can be obtained by substituting Eq. (18) into Eq. (20) and simplifying:

$$\begin{aligned} \dot{V}(x) = &\sqrt{\frac{1}{3}}\left(i_{md}^* x_3 - x_1 U_c^*\right)\frac{\Delta d}{K} \\ &+\sqrt{\frac{1}{3}}\left(i_{mq}^* x_3 - x_2 U_c^*\right)\times\frac{\Delta q}{K} - R_m\left(x_1^2 + x_2^2\right) \end{aligned} \tag{21}$$

Taking the components of the right part of Eq. (21), i.e., the ratio of the switching function fluctuations to the number of submodules is:

$$\begin{cases} \Delta d / K = \alpha\left(i_{md}^* x_3 - x_1 U_c^*\right) \\ \Delta q / K = \beta\left(i_{mq}^* x_3 - x_2 U_c^*\right) \end{cases} \tag{22}$$

where α, β are the control parameters of the Lyapunov function controller for the d, q axis.

Then the switching function of Lyapunov function control can be finally obtained as:

$$\begin{cases} S_d = S_d^* + \Delta d = \frac{K}{U_c^*}\left(U_{md} - R_m i_{md}^* + \omega_m L_{eq} i_{mq}^* - L_{eq}\frac{di_{md}^*}{dt}\right) \\ \quad +\alpha K(i_{md}^* x_3 - x_1 U_c^*) \\ S_q = S_q^* + \Delta q = \frac{K}{U_c^*}\left(U_{mq} - R_m i_{mq}^* - \omega_m L_{eq} i_{md}^* - L_{eq}\frac{di_{mq}^*}{dt}\right) \\ \quad +\beta K(i_{mq}^* x_3 - x_2 U_c^*) \end{cases} \tag{23}$$

Fig. 1 shows the Lyapunov function control box for the input side of the MMMC. Where, figure 1(a) shows the input side control frame; figure 1(b) shows the detailed control frame of Lyapunov function control. In Fig. 1(a), u_{cnN} is the average capacitance voltage of all the MMMC sub-modules, U_{dc} is the capacitance stabilized value of MMMC sub-modules, P_{mref} is the reference value of the output active power, and the output reactive power is zero.

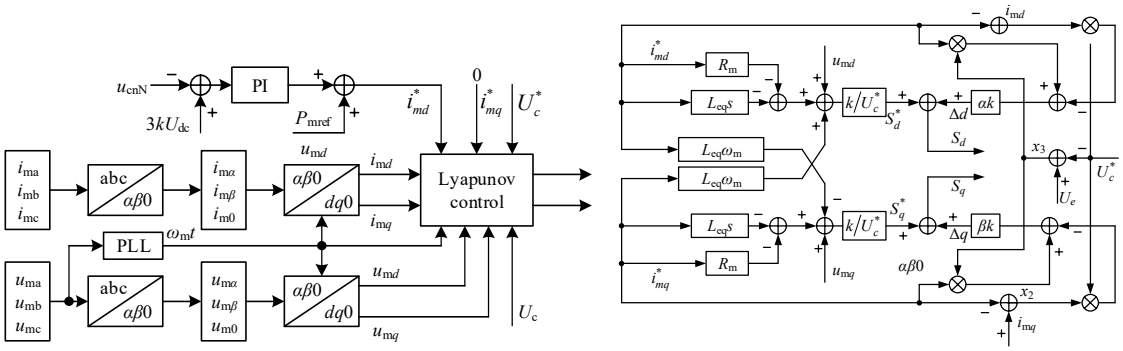

(a) Input side control block diagram (b) Lyapunov function control block diagram

Figure 1: Control block diagram of MMMC current at input side

II. C.Segmented linear approximation methods

Give a nonlinear function of the following form $g_i(z)$:

$$\sum_{i=1}^{l} g_i(z) = c \tag{24}$$

where c is a constant. For the above nonlinear function $g_i(z)$, it is proposed to approximate it by the segmented linear function method given in the following equation, which splits it into two parts: the linear function $\hat{g}_i(z)$ and the error $\Delta g_i(z)$: by using a series of linear approximations with definite vertices, the nonlinear function is approximated. According to the idea of the above method, the nonlinear function can be described in the following form:

$$g_i(z) = \sum_{k=1}^{q} \sum_{i_1=1}^{2} \cdots \sum_{i_p=1}^{2} \prod_{r=1}^{p} v_{ri_r k}(z_r)[\hat{g}_i(z_{i_1 \cdots i_p k}) + \Delta g_i(z_{i_1 \cdots i_p k})] \tag{25}$$

where, $v_{ri_r k}(z_r)$ denotes the normalized degree of affiliation function and satisfies property $0 \le v_{ri_r k}(z_r) \le 1$, $\sum_{k=1}^{q} \sum_{i_1=1}^{2} \cdots \sum_{i_p=1}^{2} \prod_{r=1}^{p} v_{ri_r k}(z_r) = 1$, $v_{ri_r=1k} = (z_r - z_{ri_r=2k}) / (z_{ri_r=1k} - z_{ri_r=2k})$, $v_{ri_r=2k} = 1 - v_{ri_r=1k}$; z_r is the rth antecedent variable, $i_r = 1,2$ are the vertices corresponding to the antecedent variable z_r in each subdomain, k denotes the the kth subdomain on the space of antecedent variables, and q is the total number of subdomains. The $\Delta g_i(z_{i_1 \cdots i_p k})$ is the estimation error of the kth subdomain satisfying $\underline{\Delta g}_i(z_{i_1 \cdots i_p k}) \le \Delta g_i(z_{i_1 \cdots i_p k}) \le \overline{\Delta g}_i(z_{i_1 \cdots i_p k})$, the constants $\overline{\Delta g}_i(z_{i_1 \cdots i_p k})$ and $\underline{\Delta g}_i(z_{i_1 \cdots i_p k})$ denote the upper and lower bounds of $\Delta g_i(z_{i_1 \cdots i_p k})$, respectively.

A function $h(x_1)$ with x_1 as the independent variable is given here, i.e., $h(x_1) = (1 - \sin^2(x_1))/4$. Linear approximation methods are applied to approximate the function $h(x_1)$.

III. Simulation experiment on control stability of nonlinear system based on Lyapunov function

In this chapter, the optimal parameters of the system controller based on Lyapunov function are determined through simulation experiments, and the event-triggered mechanism and fault scenarios are introduced to study the system control stability.

III. A. Comparison of numerical simulation of the control system with different parameters

In order to determine the optimal control parameters of the Lyapunov function controller and to improve the stability of the nonlinear system of the electrical intelligent control platform, simulation experiments are set up for two-by-two combinations between parameters α and β in different control capacitance voltages U, and the required convergence time is recorded. Table 1 summarizes the simulation results of the nonlinear system of the electrical intelligent control platform for the parameters α and β in different control U. There is a big difference in the convergence time of the Lyapunov function in the two systems X_1 and X_2 when α is taken as 0.95, 0.70, 0.45, 0.05, and β is taken as 9, 4, 2, and 1, respectively. After comparison, it can be found that the Lyapunov function has the shortest convergence time in the two systems when α is taken as 0.95 and β is taken as 9, 4, 2, and 1, respectively, and the convergence time is 2.91s-3.39s in the X_1 system and 4.35s-6.16s in the X_2 system.

Table 1: Summary of Simulation Results

α	β	X_1 Convergence time (s)	X_2 Convergence time (s)
0.95	9	3.36	6.16
0.95	4	3.39	5.21
0.95	2	3.15	5.03
0.95	1	2.91	4.35
0.70	9	3.79	6.98
0.70	4	3.36	5.83
0.70	2	3.25	5.05
0.70	1	2.84	4.41
0.45	9	4.57	8.63
0.45	4	4.34	7.44
0.45	2	4.00	6.96
0.45	1	3.91	6.05
0.05	9	5.66	13.07
0.05	4	5.54	11.21
0.05	2	5.32	10.20
0.05	1	4.85	8.92

Figure 2 demonstrates the simulation process of Lyapunov function in 2 nonlinear systems when α is taken as 0.95 and β is taken as 9, 4, 2 and 1 respectively. From the numerical simulation process with different parameters, it can be seen that when α is taken 0.95 and β is taken 2, the convergence time of the function in the 2 nonlinear systems is 3.15s and 5.03s; when α is taken 0.95 and β is taken 1, the convergence time of the function in the 2 nonlinear systems is 2.91s and 4.35s. Although the function converges the fastest when α is taken as 0.95 and β is taken as 1, the fluctuation of the convergence process is synthesized, and it is found that the fluctuation of the function convergence curve is the most gentle when α is taken as 0.95 and β is taken as 2. Therefore, in order to ensure the stable state of function convergence, this paper sets the control parameters of the Lyapunov function controller to α = 0.95, β = 2.

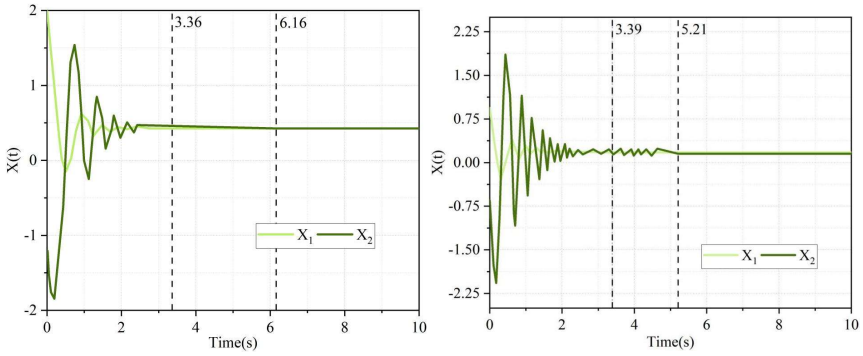

(a) α=0.95, β=9

(b) α=0.95, β=4

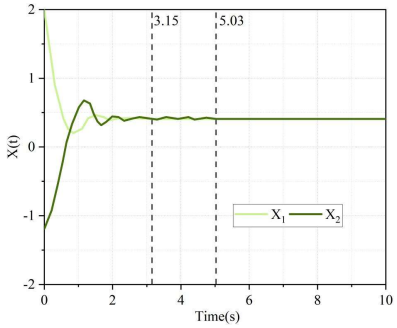

(c) α=0.95, β=2

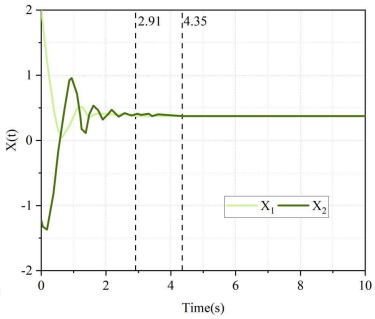

(d) α=0.95, β=1

Figure 2: Simulation process

III. B. Verification of robust stability of nonlinear system based on event-triggered mechanism

In the application of electrical intelligent control platforms, nonlinear systems are easily affected by uncertainties such as environmental perturbations and data errors, which lead to fluctuations in the parameters of the determined function controllers, resulting in a more complex dynamical behavior of the nonlinear system. In this section, based on the event-triggered sampled data control method, we verify the control stability of nonlinear systems under the control of Lyapunov-based functional controllers.

Two numerical simulation examples are designed to verify the feasibility and validity of the obtained results through the segmented linear approximation method.

Example 1: Consider the following parameter-determined nonlinear system X_1 based on event-triggered control:

$$ {}_{t_0}^{C}\mathrm{D}_t^{c(\alpha)}\mathrm{x}(t) = A\mathrm{x}(t) + Bf(\mathrm{x}(t)) + u(t), \quad t \geq 0 \tag{26} $$

where $c(\alpha) = 1*\delta(\alpha - 0.98) + 1*\delta(\alpha - 0.15)$, $f(t, \mathrm{x}(t)) = (\tanh(\mathrm{x}_1(t)), \tanh(\mathrm{x}_2(t)))^T$, $\mathrm{x}(t) = (x_1(t), x_2(t))^T$. The $\delta(\cdot)$ denotes the Dirac function.

If the system (26) has no event-triggered control inputs, i.e., the event-triggered controller $u(t) = 0$, the following parameter-determined nonlinear system can be obtained:

$$ {}_{t_0}^{C}\mathrm{D}_t^{c(\alpha)}x(t) = Ax(t) + Bf(x(t)), \quad t \geq 0 \tag{27} $$

The coefficient matrix is shown below:

$$ A = \begin{bmatrix} -4 & 3 \\ 2 & -5 \end{bmatrix}, \quad B = \begin{bmatrix} 1 & -2 \\ -3 & 2 \end{bmatrix} \tag{28} $$

Figure 3 shows the time response of the trajectory of the system state (27) without the event-triggered controller. Through numerical simulation using MATLAB mathematical software, it can be seen that the parameters of the control inputs without event triggering determine that the equilibrium point of the nonlinear system (27) fluctuates back and forth between -15-15 and is not asymptotically stable.

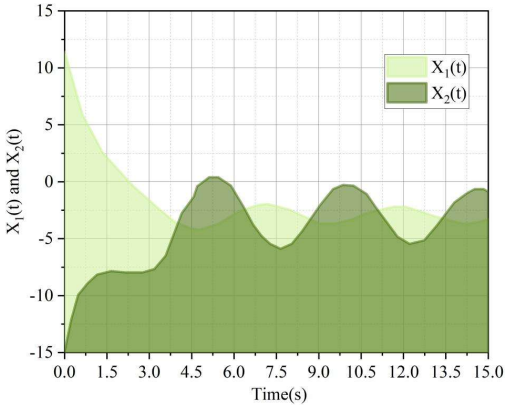

Figure 3: No event-triggered state trajectory time response of the controller

Subsequently, we consider the system (26) with an event-triggered control mechanism, and we consider the event-triggered controller to be $u(t) = Kq(t_k)$. Finally, under the event-triggered mechanism, the following nonlinear system under the control of the controller of the Lyapunov function with event-triggered control can be obtained:

$$ {}_{t_0}^{C}\mathrm{D}_t^{c(\alpha)}x(t) = (A+K)x(t) + Bf(x(t)) - Ke(t), \quad t \geq 0 \tag{29} $$

where $e(t) = x(t) - x(t_k)$. The matrix of its coefficients is shown below

$$ A = \begin{bmatrix} -4 & 3 \\ 2 & -5 \end{bmatrix}, \quad B = \begin{bmatrix} 1 & -2 \\ -3 & 2 \end{bmatrix} \tag{30} $$

Figure 4 shows the time response results of the state trajectory of the system (29) with an event-triggered controller. Numerical simulation using MATLAB mathematical software yields the equilibrium point of the nonlinear

system (29) with event-triggered Lyapunov function controller based on the event-triggered mechanism, which is asymptotically stable after 5s.

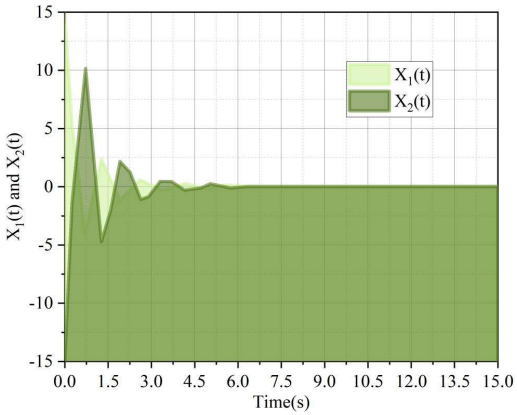

Figure 4: The state trajectory time response with an event-triggered controller

Furthermore, under the condition that Assumption 1 and Theorem 1 hold, a scalar $\varepsilon = 26.8581$ can be found such that the system can exclude Zeno behavior in the event-triggered strategy. Figure 5 shows the time series of event triggering for the system. During the event triggering time of 0-15s, the Lyapunov function controller is always outputting multiple control results. This reflects the effectiveness of the event triggering mechanism proposed in this paper, and also verifies that the design of the Lyapunov function controller of the MMMC current fully takes into account the nonlinear system disturbed by events, which can make the nonlinear system of the electrical intelligent control platform maintain good control stability.

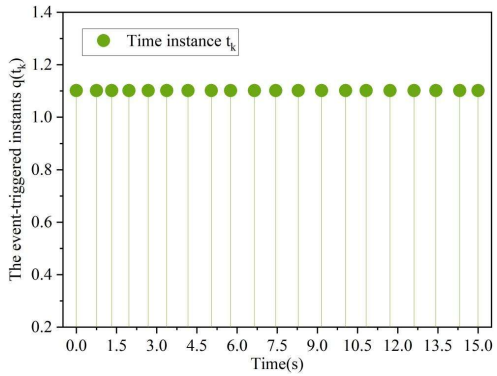

Figure 5: The instance of trigger time caused by the event-triggering mechanism

III. C. Stability analysis of system control under the influence of faults based on Lyapunov function

Fig. 6 shows the two-dimensional projections of the stability domain and the trajectory of the system state quantities on the plane (x1, x2) after the inverter-side fault is cleared for 2.5s. Fig. 7 shows the public Lyapunov function value curves after 2.5s clearing of the fault on the inverter side. Where the green circle is the position of the state vector in the space at the instant of fault clearing, the light green curve is the system motion trajectory on the state space after fault clearing, and the dark green curve is the boundary of the stabilization domain estimated by the Lyapunov function V(x) obtained iteratively. It can be clearly seen that after the inverter-side fault located at (-0.32026,-0.25566) is cleared, the system motion trajectory is able to return from the deviation position of (1.17427,3) to the vicinity of the stability domain where the dark-green curve is located, and can eventually return to the stability domain. Meanwhile, the value of the common Lyapunov function after the inverter-side fault is cleared in 2.5 s is steadily increased from the speed close to 0 to about 450.The electrical intelligent control nonlinear system under the control of the Lyapunov function controller is able to maintain stable operation even when the faults appear, and satisfies the Lyapunov stability condition, which can be well realized for the intelligent control of the electrical line.

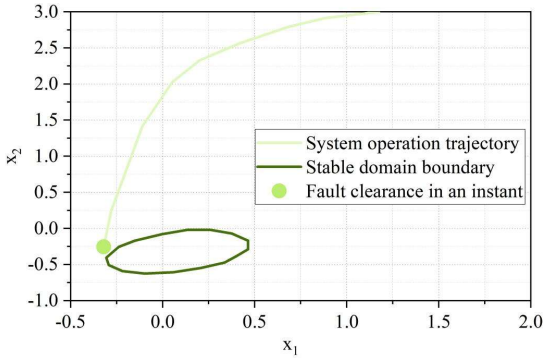

Figure 6: Two-dimensional projection

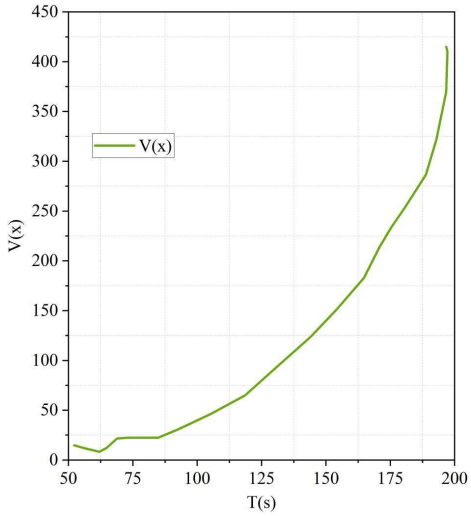

Figure 7: Public Lyapunov function value curve

IV. Conclusion

In this paper, a nonlinear system stability control method based on Lyapunov function is proposed to verify its practical effect in electrical intelligent control platform. Through simulation experiments, it is determined that the system convergence time is shorter (3.15s and 5.03s) and the convergence process is smooth when the function parameters α are taken as 0.95 and β is taken as 2. Under the event triggering mechanism, the system stabilization time using the Lyapunov function controller is around 5 seconds. Under the fault scenario, the system motion trajectory can return to the stabilization domain from the deviation position of (1.17427,3), and the value of the Lyapunov function can be steadily increased to about 450 after the fault is cleared, which provides a good stabilization control performance. In the future, the adaptive parameter adjustment mechanism can be deeply explored to improve the control effect of the nonlinear system based on Lyapunov function.

References

[1] Chen, Z., Xie, M., & Zu, Q. (2023). Electrical Automation Intelligent Control System Based on Internet of Things Technology. Electrica, 23(2).

[2] Ju, X., Gou, R., Xiao, Y., Wang, Z., & Liu, S. (2022). The use of edge computing-based internet of things big data in the design of power intelligent management and control platform. International journal of grid and utility computing, 13(1), 76-86.

[3] Ma, J. (2025). Application of intelligent technology in electrical engineering automation control. Highlights in Science, Engineering and Technology, 126, 147-150.

[4] Kaleybar, H. J., Kojabadi, H. M., Fazel, S. S., & Foiadelli, F. (2018). An intelligent control method for capacity reduction of power flow controller in electrical railway grids. Electric Power Systems Research, 165, 157-166.

[5] Wen, J., Lu, J., Zhang, S., Liu, R., Spataru, C., Weng, Y., & Lv, X. (2024). Intelligent control for rapidity and security of all-electric ships gas turbine under complex mutation load using optimized neural network. Applied Thermal Engineering, 248, 123120.

[6] Senapati, M. K., Al Zaabi, O., Al Hosani, K., Al Jaafari, K., Pradhan, C., & Muduli, U. R. (2024). Advancing electric vehicle charging ecosystems with intelligent control of DC microgrid stability. IEEE Transactions on Industry Applications.

[7] Bezpalov, V. V., Solopova, N. A., Shilina, M. G., Avtonomova, S. A., & Gorina, T. V. (2021). Formation of an intelligent control system in the field of electric power industry based on the technological development of power supply components. Periodicals of Engineering and Natural Sciences (PEN), 9(3), 218-235.

[8] Blanco, J., García, A., & Morenas, J. D. L. (2018). Design and implementation of a wireless sensor and actuator network to support the intelligent control of efficient energy usage. Sensors, 18(6), 1892.
[9] Chai, T., Li, M., Zhou, Z., Cheng, S., Jia, Y., & Wu, Z. (2023). An intelligent control method for the low-carbon operation of energy-intensive equipment. Engineering, 27, 84-95.
[10] Wu, G., & Liu, Y. (2024). Production automation and financial cost control based on intelligent control technology in sustainable manufacturing. The International Journal of Advanced Manufacturing Technology, 1-10.
[11] Arranz-Gimon, A., Zorita-Lamadrid, A., Morinigo-Sotelo, D., & Duque-Perez, O. (2021). A review of total harmonic distortion factors for the measurement of harmonic and interharmonic pollution in modern power systems. Energies, 14(20), 6467.
[12] Tang, L., Han, Y., Yang, P., Wang, C., & Zalhaf, A. S. (2022). A review of voltage sag control measures and equipment in power systems. Energy Reports, 8, 207-216.
[13] Gu, Y., Jiang, H., Zhang, J. J., Zhang, Y., Wu, H., & Muljadi, E. (2018). Multi-timescale three-phase unbalanced distribution system operation with variable renewable generations. IEEE Transactions on Smart Grid, 10(4), 4497-4507.
[14] Song, J., Zhou, X., Zhou, Z., Wang, Y., Wang, Y., & Wang, X. (2023). Review of low inertia in power systems caused by high proportion of renewable energy grid integration. Energies, 16(16), 6042.
[15] Cherukuri, A., Mallada, E., Low, S., & Cortés, J. (2017). The role of convexity in saddle-point dynamics: Lyapunov function and robustness. IEEE Transactions on Automatic Control, 63(8), 2449-2464.
[16] Sergeev, I. N. (2018). Lyapunov characteristics of oscillation, rotation, and wandering of solutions of differential systems. Journal of Mathematical Sciences, 234, 497-522.
[17] Liu, L., Liu, Y. J., Chen, A., Tong, S., & Chen, C. P. (2020). Integral barrier Lyapunov function-based adaptive control for switched nonlinear systems. Science China Information Sciences, 63, 1-14.
[18] Qiu, Z., Duan, C., Yao, W., Zeng, P., & Jiang, L. (2022). Adaptive Lyapunov function method for power system transient stability analysis. IEEE Transactions on Power Systems, 38(4), 3331-3344.